IEEE Access
Multidisciplinary | Rapid Review | Open Access Journal

Received August 3, 2019, accepted August 22, 2019, date of publication August 27, 2019, date of current version September 19, 2019.

Digital Object Identifier 10.1109/ACCESS.2019.2937835

A Broadband Tunable Coaxial Attenuator Based on Graphene

HUI CHEN, ZHEN GUO LIU, (Member, IEEE), WEI BING LU, (Member, IEEE), AN QI ZHANG, AND HAO CHEN

State Key Laboratory of Millimeter Waves, School of Information Science and Engineering, Southeast University, Nanjing 210096, China

Corresponding authors: Zhen Guo Liu (liuzhenguo@seu.edu.cn) and Wei Bing Lu (wblu@seu.edu.cn)

This work was supported in part by the National Natural Science Foundation of China (NSFC) under Grant 61671150 and Grant 61671147, and in part by the Six Talent Peaks Project in Jiangsu Province under Grant XCL-004.

ABSTRACT A dynamically tunable coaxial attenuator based on graphene is presented in this paper. The attenuator is achieved by inserting a graphene sandwich structure (GSS) inside the dielectric of coaxial line along the propagation direction of electromagnetic waves to dissipate the electromagnetic field. The mechanism of attenuator is theoretically analyzed, and an approximate formula to calculate attenuation with different parameters is proposed. We experimentally demonstrate that attenuation of the attenuator can be tuned from 3 dB to 14.5 dB with good flatness in broad operation frequency from 2 GHz to 9 GHz when graphene impedance is changed by different bias voltage. The theoretical calculation and simulation results have a good agreement with experimental results, while the $|S_{11}|$ can always remain low level under -15 dB.

INDEX TERMS Attenuator, graphene, dynamically tunable, coaxial line.

I. INTRODUCTION

Due to the advantages of single mode operation, non-dispersion, electromagnetic shielding and low loss, the coaxial transmission line is widely used in microwave devices. Accordingly, the coaxial attenuator is a critical part of the microwave circuit to diminish the signal, which can adjust the signal level to the desired value or improve the impedance matching. Considering convenient application, it is better that the attenuation of attenuator has a certain dynamically tunable range. In general, there are two main types of conventional coaxial attenuators. One is that the attenuation results from the losses of lossy medium between the inner and external conductors of coaxial lines, which is not electrically tunable generally. The other is that attenuation results from the attenuation networks on center-line circuits of coaxial systems, which can be tunable because of switches among multiple branches in circuits [1].

Graphene, as a ultra-thin two dimensional material formed by carbon atoms in honeycomb lattice, has been extensively applied in microwave devices [2]–[13]. One of the most interesting features of graphene at microwave frequency is the possibility to electronically modify its conductivity [3]–[10]. Thus the graphene, as a kind of lossy medium with electrically tunable characteristic, can be inserted between the inner and external conductors of the coaxial line to form a coaxial attenuator. Compared with two conventional coaxial attenuators, although the operation principle of the graphene-based coaxial attenuator is similar to that of the first type of coaxial attenuator, it can realize the attenuation tuning characteristic without adding any additional complex circuits into the coaxial system, such as electronic switches and attenuation networks, but only by applying bias voltage. This is quite attractive for reducing the complexity and cost of the system.

Some publications have reported the applications of the tunable conductivity of graphene in attenuators [5]–[10]. According to the influence degree of graphene on the EM wave transmission of transmission lines, the graphene-based attenuators can be classified as the transmission type and the reflection type. Reference [5] and [6] have proposed two transmission type attenuators based on graphene integrated SIW (substrate integrated waveguide) and half-mode SIW respectively. They both have satisfied tuning range and low return loss, but the performance of the attenuators in low frequency band is limited by cutoff frequency of SIW structure.

The associate editor coordinating the review of this article and approving it for publication was Flavia Grassi.

The attenuator in reference [7] as the reflection type was achieved by depositing a graphene flake on an air gap in the signal strip of a microstrip line and the attenuator in reference [10] as the transmission type placed the graphene pads between the microstrip line and ground plane, but these two attenuators, due to their relatively large return loss, may have an influence on the front-end circuit in cascade circuits.

In this paper, we proposed a broadband tunable coaxial attenuator based on graphene with low return loss. This transmission type attenuator is suitable to operate in low frequency band due to the upper cut-off frequency of coaxial line. What's more, owing to the pure TEM mode in coaxial line under cut-off frequency, the attenuator has a good flatness feature. In the proposed attenuator, the GSS is placed along the propagation direction of electromagnetic waves and employed to dissipate the transverse electric and magnetic field inside coaxial line. Since the surface impedance can be changed continuously by external bias voltage, the attenuation can be tuned accordingly.

The rest of this paper is structured in the following way. The detailed structure of the proposed graphene-based coaxial attenuator, the theoretical analysis of the attenuation and the simulated results with different critical parameters of the attenuator are presented in Section II. Subsequently, the measured results of a fabricated prototype are reported in Section III. Finally, a conclusion is drawn in Section IV.

II. THEORETICAL ANALYSIS OF GRAPHENE-BASED TUNABLE ATTENUATOR

The detailed geometry of the graphene-based coaxial attenuator is shown in Fig. 1 (a). The attenuator is composed of a coaxial line and a GSS. A GSS is a mutually gated graphene capacitor consisting of two monolayer graphene sheets supported by polyvinyl chloride (PVC) films and a diaphragm paper soaked with ion liquid electrolyte. The diaphragm paper is sandwiched between the two graphene sheets [11]. The graphene is synthesized on copper foils by chemical vapor deposition (CVD) growth approach. As shown in Fig. 2, after the growth, PVC at 150°C is laminated on the graphene-coated copper foils by roll-to-roll production method, and then the large-area monolayer graphene film on the PVC substrate is obtained by etching the copper foils with diluted nitric acid [12], [13]. R_1, R_2, R_3 are the radius of inner conductor, dielectric, external conductor of coaxial line respectively. L is the length of coaxial line. L_g is the length of the graphene sheets. The GSS is placed between the inner conductor and the external conductor, along the propagation direction of electromagnetic waves.

In light of the configuration, the attenuation results from the dissipation of TEM field inside coaxial line, which is mainly contributed by the impedance loss of GSS. Since thickness of the GSS is thin enough to be regarded as an impedance surface directly, the impedance loss of monolayer graphene inside coaxial line can be formulated by [14]:

$$p = \frac{Z_g}{2} \int_S |\vec{J}_s|^2 ds \tag{1}$$

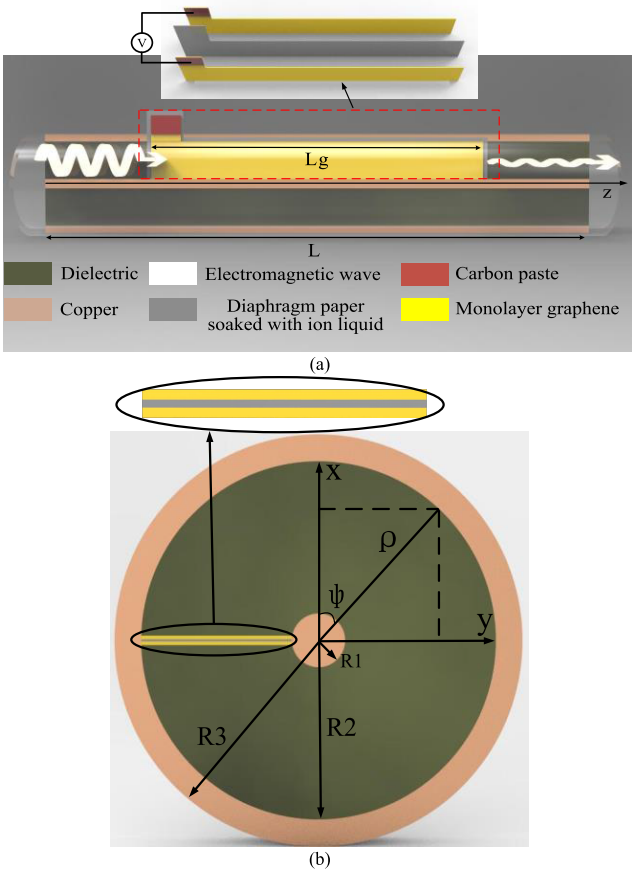

FIGURE 1. The configuration of proposed attenuator. (a) The cross section view of attenuator. (b) The side view of attenuator.

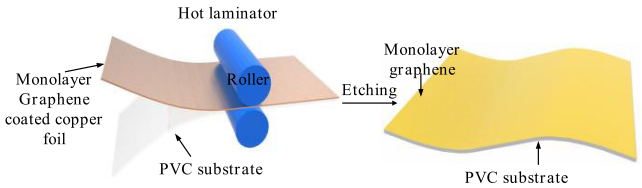

FIGURE 2. (a) The roll-to-roll production method process. (b) Large-area monolayer graphene on the PVC support.

where Z_g, J_s, S represent the surface impedance, the surface current, and the longitudinal area of GSS respectively. The surface current density can be calculated by:

$$\vec{J} = Z_g^{-1} E_\rho \hat{\rho} \tag{2}$$

where E_ρ represents the ρ-component of electric field inside coaxial line. And the electrical field can be written by:

$$\varphi(\rho, \phi) = \frac{V_o In(R_2/\rho)}{In(R_2/R_1)} \tag{3}$$

$$\vec{E} = -\nabla\varphi(\rho, \phi) \tag{4}$$

where φ represents the electric potential inside coaxial line. According to formula (3) and (4), J_s can be calculated in cylindrical coordinate system shown in Fig. 1 (b). Eventually, given the existence of two graphene monolayers in a piece of GSS, the impedance loss of graphene in the attenuator

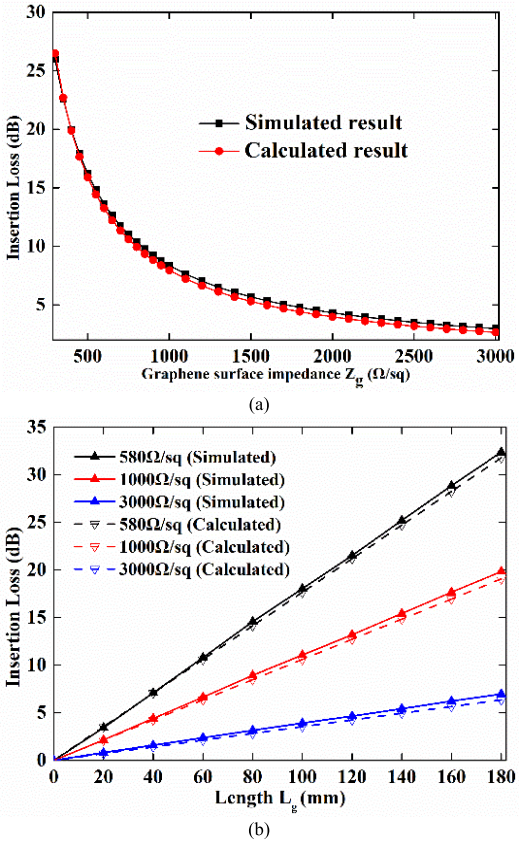

FIGURE 3. (a) The insertion loss versus the surface impedance of graphene. Squares represent the simulation results (simulated at 3 GHz) obtained by CST. Circles represent the calculated results by formula (5). ($\varepsilon_r = 1.45$, L = 200mm, L_g = 75mm, $R_1 = 2.2$mm, $R_2 = 6.25$mm, $R_3 = 6.835$mm) (b) The insertion loss versus the L_g at 3GHz. ($\varepsilon_r = 1.45$, L = 200mm, L_g = 75mm, $R_1 = 2.2$mm, $R_2 = 6.25$mm, $R_3 = 6.835$mm) The solid line with up-triangles represent the simulated results with different surface impedance. The dash line with down-triangles represent the calculated results with different surface impedance. (black-580 Ω/sq, red-1000 Ω/sq, and blue-3000 Ω/sq).

should be derived by multiplying (1) with two. Therefore, the attenuation of the attenuator can be finally expressed as:

$$P = \frac{V_o^2}{Z_g In^2(R_2/R_1)} L_g \left(\frac{1}{R_1} - \frac{1}{R_2}\right) \tag{5}$$

The principle of this attenuator can also be explained from the perspective of physics. When the surface impedance of graphene is infinitely great, the surface current equals zero, the graphene here is similar to the ideal medium. Thus the insertion loss of attenuator is almost zero. When the surface impedance gradually decreases, the surface current increases accordingly. Thus the insertion loss increases by the formula (1).

To validate the results of theoretical analysis above, CST is employed to implement the full-wave simulation of the coaxial attenuator. The attenuation P can be directly calculated by the simulation results $|S_{21}|$ according to the formula (6). The dimension of coaxial line is selected according to two conditions: 1) The characteristic impedance Z_0 of the coaxial line equals to about 50Ω to match with the feeding port.

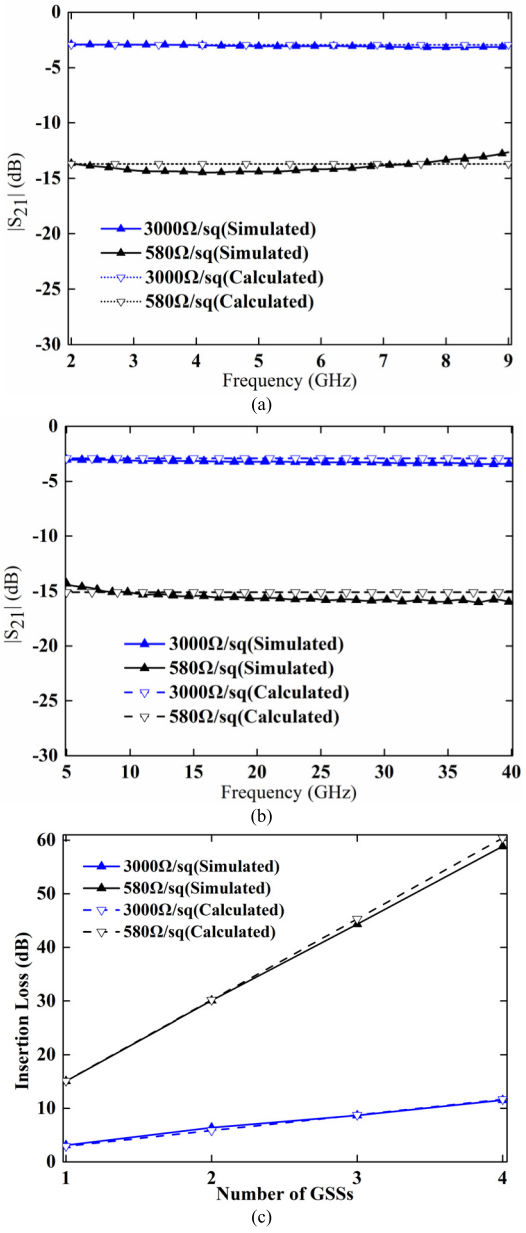

FIGURE 4. (a) $|S_{21}|$ of the proposed attenuator under the upper cut-off frequency about 9GHz with parameters as: $\varepsilon_r = 1.45$, L = 200mm, L_g = 75mm, $R_1 = 2.2$mm, $R_2 = 6.25$mm, $R_3 = 6.835$mm. (b) $|S_{21}|$ of the proposed attenuator under the upper cut-off frequency about 40GHz with parameters as: $\varepsilon_r = 1.45$, L = 50mm, L_g = 17.5mm, $R_1 = 0.5$mm, $R_2 = 1.35$mm, $R_3 = 1.935$mm. (c) Insertion loss versus the number of GSSs inserted inside the coaxial line at 9GHz. ($\varepsilon_r = 1.45$, L = 50mm, L_g = 17.5mm, $R_1 = 0.5$mm, $R_2 = 1.35$mm, $R_3 = 1.935$mm) In (a), (b) and (c), the solid line with up-triangles represent the simulated results with different surface impedance. The dash line with down-triangles represent the calculated results with different surface impedance. (black-580Ω/sq and blue-3000Ω/sq).

The characteristic impedance of coaxial line can be calculated by formula (7). 2) In order to obtain pure TEM mode in coaxial line, the operation frequency should be less than the upper cut-off frequency f_c which can be calculated by formula (8).

$$P = -20 \lg |S_{21}| \tag{6}$$

TABLE 1. Performance comparison of this work and conventional coaxial attenuators in market. The performance parameters of conventional attenuators listed below are the data from the common conventional coaxial attenuators in the market. (Type 1: A attenuator in which the attenuation is from the losses of lossy medium between the inner and external conductors of coaxial lines. Type 2 and 3: Voltage-controlled tunable coaxial attenuators in which the attenuations are from the attenuation networks on center-line circuits of coaxial systems.)

Type	$\|S_{21}\|$ range (dB)	$\|S_{11}\|$ (dB) / VSWR	Frequency band (GHz)	Structure
1	non-tunable	-- / <1.2	DC-6 / 200%	Coaxial line + lossy medium
2	40	-- / <2	0.4-6 / 175%	Coaxial system + attenuation circuits
3	37	<-5 / --	18-40 / 76%	Coaxial system + attenuation circuits
This work	11.5 (from 3dB to14.5 dB)	<-15 / --	2-9 / 127%	One GSS+coaxial line (the upper cut-off frequency is above 9GHz)
This work	12 (from 3dB to15 dB)	<-15/ --	5-40 / 156%	One GSS+coaxial line (the upper cut-off frequency is above 40GHz)
This work	48 (from 12dB to 60dB)	<-15/ --	5-40 / 156%	Four GSSs+coaxial line (the upper cut-off frequency is above 40GHz)

$$Z_0 = \sqrt{\frac{\mu}{\varepsilon}}\frac{In(R_2/R_1)}{2\pi} \tag{7}$$

where μ and ε represent the permeability and permittivity of the medium between inner and external conductor respectively.

$$f_c = \frac{c}{\pi\sqrt{\varepsilon_r}(R_1 + R_2)} \tag{8}$$

where c and ε_r represent the velocity of light in vacuum and relative dielectric constant of the medium between inner and external conductor respectively.

Fig. 3 (a) exhibits the insertion loss of attenuator at 3GHz with reference to changing surface impedance of graphene. As shown in Fig. 3 (a), there is a good agreement between simulated results and calculated results. Fig. 3 (b) shows the insertion loss of attenuator at 3GHz with reference to the changing length of graphene L_g. It can be seen that as the increase of L_g, the impedance loss of attenuator increases accordingly and the tuning range expands too, which agrees with the tendency of formula (5) indicated.

In Fig. 4 (a) and (b), $|S_{21}|$ of the proposed attenuators with different parameters under different upper cut-off frequencies are displayed. According to the simulated and calculated results, we can find that the graphene-based attenuator with one piece of the GSS has a tunable range of attenuation from 3dB to 15dB with a good flatness characteristic when the surface impedance of graphene is changed from 3000Ω/sq to 580Ω/sq, even the operation frequency up to 40GHz. Fig. 4 (c) exhibits the simulated and calculated results of insertion loss versus the number of identical GSSs paralleled with the plane of electric vectors inside the coaxial line. The results demonstrate that the insertion loss and the tunable attenuation range of the attenuator increase linearly with the number of GSSs. According to the aforementioned analysis data, the performance comparison between this work and conventional coaxial attenuators in market is listed in Table 1. When compared with common conventional coaxial attenuator, we can find that the proposed graphene-based coaxial attenuator features appropriate tunable attenuation range, low return loss and broad bandwidth, and especially with simpler structures and lower cost.

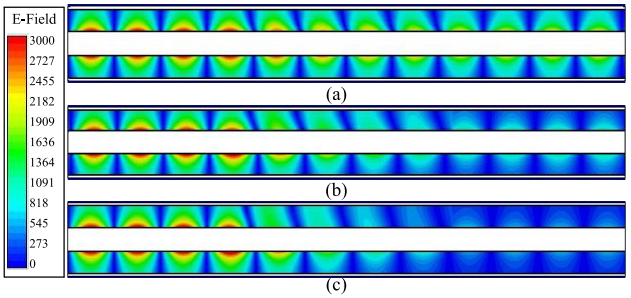

FIGURE 5. Electric field distribution of the proposed attenuator with different surface impedance of graphene (simulated at 7.5 GHz). The surface impedance of grapheme is (a) 3000Ω/sq, (b) 1000Ω/sq and (c) 580Ω/sq respectively.

Fig. 5 exhibits the electric field distribution of the proposed attenuator in the cross section with different surface impedance of graphene at 7.5GHz. In Fig. 5 (a), (b) and (c), the surface impedance of graphene is 3000Ω/sq, 1000Ω/sq, and 580Ω/sq respectively. In Fig. 5 (a), the magnitude of electric filed can be obviously observed at output port, and in Fig. 5 (c), the magnitude of electric filed can hardly be observed at output port. It can be clearly demonstrated that the magnitude of electric filed at output ports is reduced with decrease of the surface impedance of graphene, which agrees well with theoretical analysis.

III. PROTOTYPE AND EXPERIMENTAL VALIDATION

To validate the theoretical calculation and numerical simulation results, the prototype of proposed attenuator has been fabricated and measured. Before the measurement of tuning range of attenuator, the waveguide method was employed to measure the relationship between the square resistance of the graphene and bias voltage at first [15]. In Fig. 6 (a), a pair of standard waveguide was connected to a Vector Network Analyzer (VNA), and a GSS with bias voltage (the positive and negative voltages are applied to the two graphene sheets of the GSS respectively) was sandwiched between two waveguides. According to the S-parameter measured by VNA, the relationship between the square resistance and bias voltage can be obtained as shown in Fig. 6 (b). The results indicate that the square resistance of the graphene can be

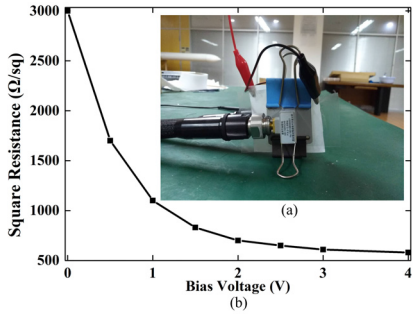

FIGURE 6. Measurement of the GSS. (a) Photograph of the GSS measurement. (b) Square resistance of graphene versus the bias voltage.

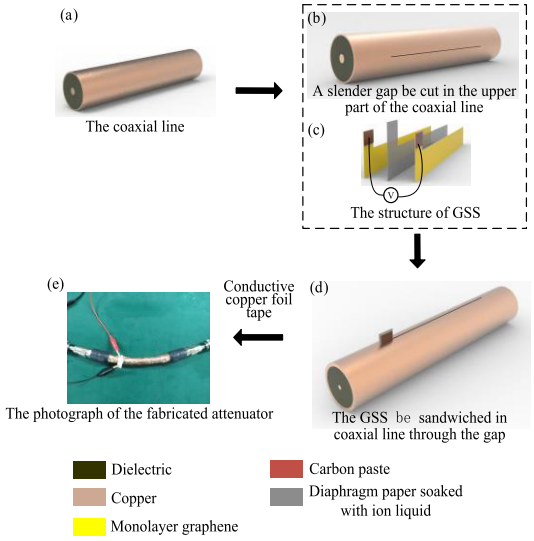

FIGURE 7. The flow chat of fabrication process of the attenuator. The parameters of the fabricated coaxial attenuator are same to one of the aforementioned simulation parameters. ($\varepsilon_r = 1.45$, $L = 200$mm, $L_g = 75$mm, $R_1 = 2.2$mm, $R_2 = 6.25$mm, $R_3 = 6.835$mm).

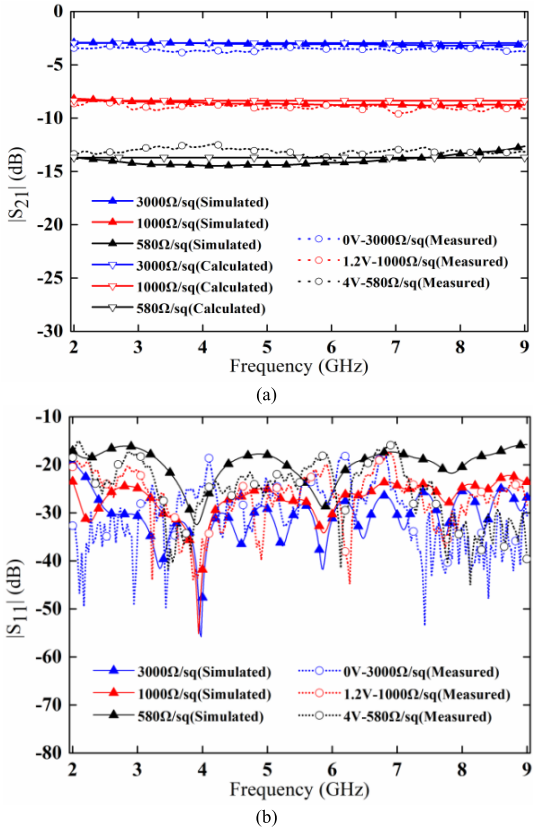

FIGURE 8. (a) The measured $|S_{21}|$ of the fabricaterd prototype. (b) The measure $|S_{11}|$ of the fabricaterd prototype. The solid line with up-triangles represent the simulated results with different surface impedance. The solid line with down-triangles represent the calculated results with different surface impedance. The dash line with circles represent the measured results. (black-580 Ω/sq, red-1000 Ω/sq, and blue-3000 Ω/sq).

tuned from 3000Ω/sq to 580Ω/sq dynamically when the bias voltage is changing from 0V to 4V. If we further increase the voltage, the surface impedance of graphene will still maintain the 580Ω/sq because of the electrochemical window of the ion liquid electrolyte, which limits the maximum charge density on graphene electrodes [11]. And the tunable behavior of the GSS is repeatable and reversible, because it is based on the electrostatic tuning of high mobility carriers on graphene electrodes, which does not damage the structure of the graphene sheets.

The flow chart of fabrication process is presented in Fig. 7. To facilitate the experiments, the coaxial line with larger radius of inner and external conductor was chosen. At first, a slender gap was cut in the upper part of the coaxial line, then the GSS was sandwiched in coaxial line through the gap. It is worth mentioning that the dimension of the diaphragm paper should be slightly larger than that of the two graphene sheets in case of a short between the two graphene sheets. After inserting the GSS into coaxial line, the conductive copper foil tape was used to stick the external conductor of coaxial line. Eventually, a prototype of the coaxial attenuator was completed as displayed in Fig. 7 (e).

The S-Parameter of the attenuator was measured with a VNA, and a 2400 Source Meter was employed to bias graphene. The detailed tuning process is that we change the bias voltage from 0V to 4V by adjusting the 2400 Source Meter to get dynamically tunable attenuation of the attenuator which results from the tunable surface impedance of the GSS by different bias voltages. The operation frequency is from 2GHz to 9GHz. Fig. 8 (a) displays the measured, simulated and calculated results of $|S_{21}|$ of attenuator with different surface resistance of graphene. It can be clearly demonstrated that the attenuator has a tuning range of attenuation from 3dB to 14.5dB. Besides, the measured response time between the maximum and minimum attenuation is around 800ms, which is on the same time-scale as that in [11]. And in measured results, amplitude of $|S_{21}|$ with a fixed graphene impedance fluctuate within 1dB, which indicates the proposed attenuator has a good flatness characteristic in operation frequency. Fig. 8 (b) displays the measured and simulated results of $|S_{11}|$ of attenuator corresponding to different surface resistance of graphene in operation frequency. It can be seen that the $|S_{11}|$ can always remain

TABLE 2. Performance comparison of this work and previously reported graphene-based tunable attenuators.

Ref.	$\|S_{21}\|$ range (dB)	Flatness (dB)	$\|S_{11}\|$ (dB)	Frequency band (GHz) / relative bandwidth	Structure	Graphene-based attenuation type
Ref. 5	3-15	3.5	<-14	7-14.5 / 69.8%	Graphene sheet+SIW	Transmission
Ref. 6	3-14	1.8	<-20	7.7-19 / 84.6%	Graphene sheet+half-mode SIW	Transmission
Ref. 7	3-9.5	2	<-5	2-5 / 85.7%	Graphene flake+microstrip line	Reflection
Ref. 10	0.3-14	2	<-5	0-5 / 200%	Graphene flake+microstrip line	Transmission
This work	3-14.5	1	<-15	2-9 / 127.3%	Graphene sheet+coaxial line	Transmission

low level under −15 dB. It is worth mentioning that the experimental results of S-parameter have a good agreement with the theoretical calculation and numerical simulation results in frequency band. The minor differences between measured results, simulated results and calculated results may be induced by fabrication tolerance and the SMA connectors. What's more, the performance comparison between this work and previously reported graphene-based tunable attenuators is also listed in Table 2. It can be obviously seen that the proposed coaxial attenuator has the characteristic of broad bandwidth, appropriate tunable range, good flatness and low return loss when compared with other graphene-based attenuators in the Table 2.

IV. CONCLUSION

A dynamically tunable coaxial attenuator based on graphene is presented in this paper. The attenuator is achieved by the graphene sheets placed between the inner and external conductors along the direction of electromagnetic waves propagation to dissipate EM field inside coaxial line. Theoretical analysis is presented and a closed formula is given to calculate the attenuation of attenuator with different parameters. The influence of surface impedance Z_g, the length L_g, and the number of GSSs on the insertion loss are demonstrated in detail by theoretical calculation and numerical simulation. To validate the calculation and simulation results, a coaxial attenuator has been fabricated with desired attenuation and operation frequency band, and the measured results agree well with calculated and simulated results. The measured results of the fabricated attenuator manifest that the attenuation with good flatness feature can be tuned from 3dB to 14.5dB in operation frequency from 2GHz to 9GHz with low return loss. The proposed graphene-based coaxial attenuator has potential instead of conventional coaxial attenuators for effective and wide utilization in microwave systems.

REFERENCES

[1] D. Russell and W. Larson, "RF attenuation," *Proc. IEEE*, vol. 55, no. 6, pp. 942–959, Jun. 1967.
[2] K. Byun, Y. J. Park, J.-H. Ahn, and B.-W. Min, "Flexible graphene based microwave attenuators," *Nanotechnology*, vol. 26, no. 5, Jan. 2015, Art. no. 055201.
[3] E. O. Polat, O. Balcı, and C. Kocabas, "Graphene based flexible electrochromic devices," *Sci. Rep.*, vol. 4, Oct. 2014, Art. no. 6484.
[4] M. Bozzi, L. Pierantoni, and S. Bellucci, "Applications of graphene at microwave frequencies," *Radioengineering*, vol. 24, no. 3, pp. 661–669, Sep. 2015.
[5] A.-Q. Zhang, W.-B. Lu, Z.-G. Liu, H. Chen, and B.-H. Huang, "Dynamically tunable substrate-integrated-waveguide attenuator using graphene," *IEEE Trans. Microw. Theory Techn.*, vol. 66, no. 6, pp. 3081–3089, Jun. 2018.
[6] A. Zhang, Z. Liu, W. Lu, and H. Chen, "Graphene-based dynamically tunable attenuator on a half-mode substrate integrated waveguide," *Appl. Phys. Lett.*, vol. 112, no. 16, 2018, Art. no. 161903.
[7] L. Pierantoni, D. Mencarelli, M. Bozzi, R. Moro, S. Moscato, L. Perregrini, F. Micciulla, A. Cataldo, and S. Bellucci, "Broadband microwave attenuator based on few layer graphene flakes," *IEEE Trans. Microw. Theory Techn.*, vol. 63, no. 8, pp. 2491–2497, Aug. 2015.
[8] L. Pierantoni, D. Mencarelli, M. Bozzi, R. Moro, and S. Bellucci, "Graphene-based electronically tunable microstrip attenuator," in *IEEE MTT-S Int. Microw. Symp. Dig.*, Tampa, FL, USA, Jun. 2014, pp. 1–3.
[9] L. Pierantoni, M. Bozzi, R. Moro, D. Mencarelli, and S. Bellucci, "On the use of electrostatically doped graphene: Analysis of microwave attenuators," in *Proc. IEEE Int. Conf. Numer. Electromagn. Modeling Optim. RF, Microw., THz. Appl. (NEMO)*, Pavia, Italy, May 2014, pp. 1–4.
[10] M. Yasir, S. Bistarelli, A. Cataldo, M. Bozzi, L. Perregrini, and S. Bellucci, "Enhanced tunable microstrip attenuator based on few layer graphene flakes," *IEEE Microw. Wireless Compon. Lett.*, vol. 27, no. 4, pp. 332–334, Apr. 2017.
[11] O. Balci, E. O. Polat, N. Kakenov, and C. Kocabas, "Graphene-enabled electrically switchable radar-absorbing surfaces," *Nature Commun.*, vol. 6, Mar. 2015, Art. no. 6628.
[12] H. Chen, W.-B. Lu, Z.-G. Liu, J. Zhang, A.-Q. Zhang, and B. Wu, "Experimental demonstration of microwave absorber using large-area multilayer graphene-based frequency selective surface," *IEEE Trans. Microw. Theory Techn.*, vol. 66, no. 8, pp. 3807–3816, Aug. 2018.
[13] H. Chen, Z.-G. Liu, W.-B. Lu, A.-Q. Zhang, X.-B. Li, and J. Zhang, "Microwave beam reconfiguration based on graphene ribbon," *IEEE Trans. Antennas Propag.*, vol. 66, no. 11, pp. 6049–6056, Nov. 2018.
[14] D. M. Pozar, *Microwave Engineering*. New York, NY, USA: Wiley, 1998.
[15] J. S. Gómez-Díaz, J. Perruisseau-Carrier, P. Sharma, and A. Ionescu, "Non-contact characterization of graphene surface impedance at micro and millimeter waves," *J. Appl. Phys.*, vol. 111, May 2012, Art. no. 114908.

HUI CHEN was born in Jiangsu, China. She received the B.S. degree from Soochow University, Suzhou, China, in 2017. She is currently pursuing the M.S. degree in electromagnetic field and microwave technology with Southeast University, Nanjing, China. Her current research interests include antenna design and graphene applications.

ZHEN GUO LIU was born in Jiangsu, China. He received the B.S. degree from Soochow University, Suzhou, China, in 1996, and the M.S. and Ph.D. degrees from Southeast University, Nanjing, China, in 2002 and 2013, respectively. From 2005 to 2006, he was a Visiting Scholar with the Department of Electronic and Telecommunication, Politecnico di Torino, Italy. From 2011 to 2012, he was a Research Staff Member with the Department of Electrical and Computer Engineering, National University of Singapore, Singapore. From 2014 to 2015, he was a Postdoctoral Visitor with the Department of Electrical and Computer, University of Houston. Since 2002, he has been with the School of Information Science and Engineering, Southeast University, where he is currently an Associate Professor. His current research interests include graphene applications, antenna theory and application, wearable functional devices, and metamaterial antenna.

WEI BING LU was born in Jiangsu, China, in 1977. He received the B.S. and M.S. degrees from Northeast Normal University, Changchun, China, in 1999 and 2002, respectively, and the Ph.D. degree from Southeast University, Nanjing, China. He joined the State Key Laboratory of Millimeter Waves, Southeast University, in 2005, and he was promoted to an Associate Professor and a Professor, in 2006 and 2008, respectively. In 2013, he visited the ECE Department, University of California San Diego (UCSD) as a Visiting Scholar, supported by the Huaying Education and Culture Foundation. He is currently the Vice Dean of the School of Information Science and Technology, Southeast University. He has authored or coauthored over 40 journal publications. His research interests include computational electromagnetic and fast algorithms, and electromagnetic compatibility (EMC). Very recently, he was interested in graphene-based microwave devices, such as absorbers, attenuator, and antennas.

He received a young scholarship from the Huaying Education and Culture Foundation, in 2007. He received an Award of the Excellent Ph.D. Dissertation of Jiangsu Province, in 2006, a New Century Excellent Scholar Award from the Chinese Ministry of Education, in 2008, and an Award of Six Talent Peaks Project in Jiangsu Province, in 2016.

AN QI ZHANG is currently pursuing the Ph.D. degree with the School of Information Science and Engineering, Southeast University, Nanjing, China. Her current research interests include microwave and millimeter-wave transmission line, and components based on graphene.

HAO CHEN was born in Anqing, Anhui, China, in 1993. He received the B.S. degree from Dalian Maritime University, Liaoning, China, in 2015. He is currently pursuing the doctoral degree with the School of Information Science and Engineering, Southeast University, Nanjing, China. His research interests include the graphene-based absorbers and graphene-based reflect-arrays.